DMD Fast Forward. Published on May 6, 2021 as DOI: 10.1124/dmd.120.000315
This article has not been copyedited and formatted. The final version may differ from this version.

Title Page

Improving the Translation of Organic Anion Transporting Polypeptide Substrates using HEK293 Cell Data in the Presence and Absence of Human Plasma via PBPK Modeling

Christine M. Bowman, Buyun Chen, Jonathan Cheong, Liling Liu, Yuan Chen, Jialin Mao

Department of Drug Metabolism and Pharmacokinetics, Genentech, Inc., South San Francisco, CA 94080 (CMB, BC[#], JC, LL, YC, JM)

[#]Present Address: AstraZeneca, South San Francisco, CA

DMD Fast Forward. Published on May 6, 2021 as DOI: 10.1124/dmd.120.000315
This article has not been copyedited and formatted. The final version may differ from this version.

Running Title Page

Running Title: PBPK Modeling of OATP Substrates with HEK293 Data +/- Plasma

Corresponding authors:

Jialin Mao, PhD
Department of Drug Metabolism and Pharmacokinetics, Genentech, Inc., South San Francisco, CA 94080
Tel: 650-467-7061; mao.jialin@gene.com

Christine Bowman, PhD (co-corresponding author)
Department of Drug Metabolism and Pharmacokinetics, Genentech, Inc., South San Francisco, CA 94080
Tel: 650-225-6301; bowman.christine@gene.com

Text pages: 19
Tables: 5
Figures: 2
References: 73
Words in Abstract: 209
Words in Introduction: 646
Words in Discussion: 1499

Abbreviations:

AUC, area under the concentration-time curve; BCRP, breast cancer resistance protein; $CL_{int,T}$, intrinsic clearance; CL_{PD}, passive diffusion; C_{max}, maximal concentration; CYP, cytochrome P450; DDI, drug-drug interaction; fu_p, fraction unbound in plasma; HEK, human embryonic kidney; IV, intravenous; IVIVE, in vitro - in vivo extrapolation; MRP, multidrug resistance-associated protein; OATP, organic anion transporting polypeptide; PBPK, physiologically based pharmacokinetic; PK, pharmacokinetic; PO, oral; REF, relative expression factor; SCHH, sandwich cultured human hepatocytes; t_{max}, time to the maximal concentration; V_{ss}, volume of distribution

DMD Fast Forward. Published on May 6, 2021 as DOI: 10.1124/dmd.120.000315
This article has not been copyedited and formatted. The final version may differ from this version.

Abstract

Accurately predicting the pharmacokinetics of compounds that are transporter substrates has been notoriously challenging using traditional in vitro systems and physiologically based pharmacokinetic (PBPK) modeling. The objective of this study was to use PBPK modeling to understand the translational accuracy of data generated with human embryonic kidney (HEK)293 cells overexpressing the hepatic uptake transporters OATP1B1/3 with and without plasma, while accounting for transporter expression. Models of four OATP substrates, two with low protein binding (pravastatin and rosuvastatin) and two with high protein binding (repaglinide and pitavastatin) were explored, and the OATP in vitro data generated in plasma incubations were utilized for a plasma model, and in buffer incubations for a buffer model. The pharmacokinetic parameters and concentration-time profiles of pravastatin and rosuvastatin were similar and well-predicted (within two-fold of observed values) using the plasma and buffer models without needing an empirical scaling factor, while the dispositions of the highly protein bound repaglinide and pitavastatin were more accurately simulated with the plasma models than the buffer models. This work suggests that data from HEK293 overexpressing transporter cells corrected for transporter expression represents a valid approach to improve bottom-up PBPK modeling for highly protein bound OATP substrates with plasma incubations and low protein binding OATP substrates with or without plasma incubations.

Significance Statement: This work demonstrates the bottom-up approach of using in vitro data directly without employing empirical scaling factors to predict the IV PK profiles reasonably well for four OATP substrates. Based on these results, using HEK293 overexpressing cells, examining the impact of plasma for highly bound compounds, and incorporating transporter

DMD Fast Forward. Published on May 6, 2021 as DOI: 10.1124/dmd.120.000315
This article has not been copyedited and formatted. The final version may differ from this version.

quantitation for the lot in which the in vitro data were generated represents a valid approach to achieve more accurate prospective PK predictions for OATP substrates.

DMD Fast Forward. Published on May 6, 2021 as DOI: 10.1124/dmd.120.000315
This article has not been copyedited and formatted. The final version may differ from this version.

Introduction

Investigating the role of transporters during drug discovery and development is crucial as they can impact not only a drug's pharmacokinetic (PK) profile, but also its target tissue exposure and pharmacological/toxicological effect (Giacomini et al., 2010). Two commonly examined transporters, organic anion transporting polypeptide (OATP)1B1 and OATP1B3, are hepatic basolateral uptake transporters whose clinical importance has been demonstrated in both genetic studies (Niemi et al., 2005; Zhang et al., 2006; Pasanen et al, 2007) and drug-drug interaction (DDI) studies (Backman et al., 2002; Kyrklund et al., 2003; Simonson et al., 2004). As these interactions can lead to dose adjustments, and even drug withdrawals due to safety, regulatory agencies recommend evaluating drug candidates for their potential to be OATP1B1/3 inhibitors and substrates (if eliminated by the liver).

An increasingly used approach to mechanistically predict PK and transporter-mediated drug disposition is physiologically based pharmacokinetic (PBPK) modeling (Rostami-Hodjegan, 2012). In contrast to static methods where an in vitro parameter is used to predict a specific PK parameter, PBPK modeling is dynamic and can be used to predict the plasma concentration-time curve as well as time-varying changes in transporter uptake and inhibition (Sager et al., 2015). However, there have been challenges with the in vitro to in vivo extrapolation (IVIVE) of transporter kinetics to describe observed PK or DDI data, leading to the inclusion of compound-dependent empirical scaling factors in PBPK models beyond physiological scaling (Jones et al., 2012; Li et al., 2014). For instance, reported PBPK models of well-known OATP substrates pravastatin, rosuvastatin, repaglinide, and pitavastatin needed to use empirical scaling factors when inputting in vitro hepatocyte data in order to capture the observed PK (Varma et al., 2012; Jones et al., 2012; Varma et al., 2013; Duan et al., 2017).

DMD Fast Forward. Published on May 6, 2021 as DOI: 10.1124/dmd.120.000315
This article has not been copyedited and formatted. The final version may differ from this version.

To improve transporter IVIVE, recommendations have included finding in vitro systems that are more relevant to in vivo, and accounting for transporter differences between in vitro systems and in vivo (Grimstein et al., 2019; Taskar et al., 2019). To more accurately capture in vivo kinetics, the addition of plasma to in vitro incubations has been explored, and a previous study using uptake data from plateable human hepatocytes in human plasma demonstrated that the concentration-times profiles of pravastatin could successfully be captured with PBPK modeling without an empirical scaling factor (Mao et al., 2018). A recent publication also found that including serum in human and monkey hepatocyte incubations decreased the empirical scaling factor values needed to capture in vivo uptake clearance (Liang et al., 2020). To bridge the difference in transporter expression levels between different in vitro systems (such as human embryonic kidney (HEK)293 cells and hepatocytes) and/or between in vitro and in vivo (such as hepatocytes and liver tissue), the use of a relative expression factor (REF) has been proposed with transporter abundance differences measured with LC-MS/MS (Bosgra et al., 2014, Chan et al., 2019). Using this approach, Ishida et al. (2018) found that the uptake clearance of rosuvastatin in rats could be accurately predicted using Oatp-overexpressing cells and REF, while using sandwich cultured rat hepatocytes led to underprediction.

The objective of the current work is to understand the translational accuracy of using data generated in HEK293 cells overexpressing OATP1B1/3 with and without plasma, and using in-house transporter quantitation data for REF, as inputs for the PBPK models of pravastatin, rosuvastatin, repaglinide, and pitavastatin. The uptake clearance measured with this in vitro data is compared to the previously fitted uptake clearance values from PBPK models, and predictions of pharmacokinetic parameters and concentration-time profiles are examined. While many have used hepatocytes for transporter IVIVE (Izumi et al., 2017), using transporter overexpressing

DMD Fast Forward. Published on May 6, 2021 as DOI: 10.1124/dmd.120.000315
This article has not been copyedited and formatted. The final version may differ from this version.

cells may be preferable due to information about specific transporter contributions, lack of lot variability, and cost (Kumar et al., 2020). Finding an appropriate in vitro system and incubation conditions is crucial for more accurate prospective PK predictions, and may avoid the previously needed compound-specific empirical scaling factors.

Methods

Uptake in OATP1B1- and OATB1B3-Overexpressing Cells

Details on the in vitro data generation can be found in Bowman et al. (2020). Briefly, Corning TransportoCells™ Cryopreserved SLC Transporter Cells (human OATP1B1*1a OATP1B3 (lot 5278015), and control cells (lot 6075312) were used to measure the uptake of four OATP substrates (pravastatin, rosuvastatin, repaglinide, and pitavastatin) at various concentrations using protein-free buffer or 100% human plasma. Plasma protein binding of the compounds was measured with a Rapid Equilibrium Dialysis Plate (Thermo Fisher Scientific, Waltham, MA). The resulting unbound K_m, J_{max}, and passive diffusion (CL_{PD}) values can be found in Table 1. The CL_{PD} values were later converted from the original units of μL/min/mg protein to mL/min/10^6 HEK293 cells for the simulator required input of mL/min/10^6 hepatocytes. The surface area, membrane composition etc. of HEK293 cells and hepatocytes were assumed to be similar to allow for the passive diffusion in HEK293 cells to be input here as a hepatocyte value.

Transporter Quantification in Overexpressing Cell Lines and Human Hepatocytes

ProteoExtract® native membrane protein extraction kit (Millipore) was used to isolate membrane proteins from the Corning TransportoCells™ Cryopreserved SLC Transporter Cells

DMD Fast Forward. Published on May 6, 2021 as DOI: 10.1124/dmd.120.000315
This article has not been copyedited and formatted. The final version may differ from this version.

mentioned above and suspended human hepatocytes (BioIVT Corp, Westbury, NY, 10-donor pooled) according to the protocol provided by the manufacturer. 20 µL of the extracted membrane fraction were mixed with 80 µL 5% DOC (deoxycholate) in 25mM Ammonium Bicarbonate. DOC was then removed by desalting spin column after DTT (Dithiothreitol) reduction and IAA (iodoacetamide) alkylation. Trypsin was then added to each well in an enzyme to protein ratio of 1:20. Samples were digested at 37°C overnight. Heavy labeled peptides were spiked into the digestion mixture and the reaction was quenched with 0.5% of formic acid for LC-MS analysis. The surrogate peptides measured were ITPTDSR, NVTGFFQSFK, YVEQQYGQPSSK, and SSSGNK for OATP1B1 and NQTANLTNQGK, NVTGFFQSLK, and IYNSVFFGR for OATP1B3. The LC-MS analysis was carried out on a Shimadzu Nexera (Columbia, MD) coupled to a Sciex QTRAP® 6500 mass spectrometer (Foster City, CA). A Waters XBridge BEH C18 column (100 × 2.1 mm, 3.5 µm) (Milford, MA) was used with H2O (A) and MeOH (B) both with 0.1% formic acid. Gradient elution profile at 300 µL/min and 40°C is as follows: 5% B increased to 50% B by 45.0 min, then to 90% B by 50 min, and returning to 5% B at 51 min with run time of 60 min. The calibration curve range was 0.12-30 ng/mL for each peptide.

Relative Expression Factor Scaling

The transporter quantitation results were used to account for abundance differences between the overexpressing HEK293 cells and hepatocytes in the form of REF. REF is traditionally a unitless scalar, for instance correcting for pmol/10^6 cells in vivo vs. in vitro; however here for the correction of abundance in HEK293 cells vs. hepatocytes, the quantitation of HEK293 cells was measured as pmol/mg protein, leading to REF with units of mg/10^6 cells.

DMD Fast Forward. Published on May 6, 2021 as DOI: 10.1124/dmd.120.000315
This article has not been copyedited and formatted. The final version may differ from this version.

Since the mg protein/10^6 cells is not necessarily the same for HEK293 cells and hepatocytes, this has been normalized in the REF equation (Equation 1). The amount of protein was determined using the Pierce™ BCA® Protein Assay Kit (Thermo Fisher Scientific, Waltham, MA). The scaled uptake $CL_{int,T}$ is shown is Equation 2.

$$REF\ (mg/10^6\ cells) = \frac{hepatocyte\ OATPx\ abundance\ (pmol/10^6\ cells)}{HEK293\ OATPx\ abundance\ (pmol/mg\ protein)} * \frac{mg\ protein/10^6\ cells\ (hepatocytes)}{mg\ protein/10^6\ cells\ (HEK293)} \quad (1)$$

HEK293 $CL_{int,T}$ (uL/min/10^6 cells) = (J_{max} (pmol/min/mg)/ $K_{m,u}$ (uM)) * REF (mg/10^6 cells) (2)

PBPK Models of Four OATP Substrates

The Simcyp® simulator (Version 19 release 1, Sheffield, UK) was utilized for this investigation along with the models of pravastatin, rosuvastatin, and repaglinide in the Simcyp compound library and the model of pitavastatin from Duan et al. (2017). These models are considered the base models. While further development can be done as recently described for rosuvastatin (Bowman et al., 2020), the purpose of this exercise was to compare the simulation results when using the currently investigated HEK293 cell data with in house REF (and unchanged remaining model inputs) to the simulation results of the base models.

The models of pravastatin, rosuvastatin, and pitavastatin used the Advanced Dissolution, Absorption, and Metabolism (ADAM) model (Jamei et al., 2009) to describe intestinal absorption while repaglinide used the first-order absorption model. For distribution, all four compounds used a full PBPK model and the volume of distribution (V_{ss}) was predicted using the Rodgers and Rowland (2007) method. Permeability-limited models were used in the intestine for pravastatin and rosuvastatin; in the liver for all four compounds, and in the kidney for pravastatin. Details about the model inputs for these four compounds in the base models,

DMD Fast Forward. Published on May 6, 2021 as DOI: 10.1124/dmd.120.000315
This article has not been copyedited and formatted. The final version may differ from this version.

HEK293 plasma models, and HEK293 buffer models are summarized in Table 2 and briefly described below.

Pravastatin

Base model (Simcyp simulator version 19 library file): Pravastatin is a low protein binding statin (fraction unbound in plasma (fu_p)=0.485)) that is minimally metabolized and undergoes biliary and renal clearance (Singhvi et al., 1990). To assign hepatic uptake contributions in the model of pravastatin, a global hepatic uptake intrinsic clearance ($CL_{int,T}$) was back-calculated by fitting clinical IV data (Singhvi et al., 1990). The percentage of OATP1B1 and OATP1B3 contribution was then assigned based on data from HEK293-OATP1B1 and OATP1B3 cells along with relative expression data (Simcyp, 2020). The passive diffusion was measured in sandwich cultured human hepatocytes (SCHH) (Jones et al., 2012). The hepatic efflux transporter multidrug resistance-associated protein (MRP)2 was assigned using a measured $CL_{int,T}$ from sandwich culture human hepatocytes (Jones et al., 2012) and a REF was included to account for abundance differences (Neuhoff et al., 2013).

HEK293 plasma model: The hepatic OATP1B1 inputs (J_{max}, K_m, REF), OATP1B3 inputs (J_{max}, K_m, REF), and CL_{PD} inputs were updated with the in vitro results of Table 1. The remaining parameters were kept the same as the base model.

HEK293 buffer model: The hepatic OATP1B1 inputs (J_{max}, K_m, REF), OATP1B3 inputs (J_{max}, K_m, REF), and CL_{PD} inputs were updated with the in vitro results of Table 1. The remaining parameters were kept the same as the base model.

Rosuvastatin

DMD Fast Forward. Published on May 6, 2021 as DOI: 10.1124/dmd.120.000315
This article has not been copyedited and formatted. The final version may differ from this version.

Base model (Simcyp simulator version 19 library file): Rosuvastatin is a relatively low protein binding statin (fu_p=0.107) that is minimally metabolized and predominately undergoes biliary and renal excretion unchanged (Martin et al., 2003b; Bergman et al., 2006). Since inputting experimental transporter data in the rosuvastatin model could not capture the observed profile (Jamei et al., 2014), a global intrinsic clearance for active hepatic uptake was back-calculated using an IV clinical study (Martin et al., 2003a) and in vitro data was used to assign a percentage contribution to each hepatic uptake transporter included (OATP1B1, OATP1B3, OATP2B1, NTCP) based on a meta-analysis of data (Harwood et al., manuscript in preparation). The passive diffusion input was based on a meta-analysis of 5 SCHH studies. For the hepatic efflux transporter breast cancer resistance protein (BCRP), sandwich culture human hepatocyte data was input with activity corrections for absolute abundance (Li et al., 2009, Burt et al., 2016). Multidrug resistance-associated protein (MRP)4 was assigned using a relationship between rosuvastatin's hepatocyte basolateral efflux and biliary clearance (Pfeifer et al., 2013) and correcting transporter expression differences (Harwood et a., manuscript in preparation).

HEK293 plasma model: The hepatic OATP1B1 inputs (J_{max}, K_m, REF), OATP1B3 inputs (J_{max}, K_m, REF), and CL_{PD} inputs were updated with the in vitro results of Table 1. The remaining parameters were kept the same as the base model.

HEK293 buffer model: The hepatic OATP1B1 inputs (J_{max}, K_m, REF), OATP1B3 inputs (J_{max}, K_m, REF), and CL_{PD} inputs were updated with the in vitro results of Table 1. The remaining parameters were kept the same as the base model.

Repaglinide

DMD Fast Forward. Published on May 6, 2021 as DOI: 10.1124/dmd.120.000315
This article has not been copyedited and formatted. The final version may differ from this version.

Base model (Simcyp simulator version 19 library file): Repaglinide, a high protein binding anti-diabetic drug (fu_p=0.0188), is extensively metabolized by cytochrome P450 (CYP) 2C8 and CYP3A4 in the liver and gastrointestinal tract (Bidstrup et al., 2003). In the repaglinide model, hepatic uptake clearance was assigned to OATP1B1 after fitting clinical oral data (Kajosaari et al., 2005). The passive diffusion was measured in SCHH (Jones et al., 2012).

HEK293 plasma model: The hepatic OATP1B1 inputs (J_{max}, K_m, REF) and CL_{PD} inputs were updated with the in vitro results of Table 1. The remaining parameters were kept the same as the base model.

HEK293 buffer model: The hepatic OATP1B1 inputs (J_{max}, K_m, REF) and CL_{PD} inputs were updated with the in vitro results of Table 1. The remaining parameters were kept the same as the base model.

Pitavastatin

Base model (Duan et al. (2017)): Pitavastatin is a highly protein bound statin (fu_p=0.005) that undergoes minimal metabolism and is eliminated unchanged in the bile (Hirano et al., 2005). The model developed by Duan et al. (2017) was utilized as a base model here, and for hepatic uptake, OATP1B1 and OATP1B3 $CL_{int,T}$ values generated in hepatocytes were input (Hirano et al., 2006). However, this led to underprediction of the systemic clearance, so empirical scaling factors of 18 for both transporters were then included based on optimization with IV and oral clinical data (FDA). A passive diffusion value was input from the same source based on hepatocyte data (Hirano et al., 2006).

DMD Fast Forward. Published on May 6, 2021 as DOI: 10.1124/dmd.120.000315
This article has not been copyedited and formatted. The final version may differ from this version.

HEK293 plasma model: The hepatic OATP1B1 inputs (J_{max}, K_m, REF), OATP1B3 inputs (J_{max}, K_m, REF), and CL_{PD} inputs were updated with the in vitro results of Table 1. The remaining parameters were kept the same as the base model.

HEK293 buffer model: The hepatic OATP1B1 inputs (J_{max}, K_m, REF), OATP1B3 inputs (J_{max}, K_m, REF), and CL_{PD} inputs were updated with the in vitro results of Table 1. The remaining parameters were kept the same as the base model.

PBPK Model Simulations

For each compound, an intravenous (IV) and oral (PO) PK simulation was conducted using the Simcyp simulator version 19 with the Sim-Healthy Volunteer population and compared to the observed clinical data. The OATP1B1/3 abundance in liver tissue was left as the simulator default values which are from a meta-analysis (Burt et al., 2016). Details of the clinical studies and the exact simulations run (number of subjects, age range, and proportion of females) can be found in Table 3. Ten trials were run for each simulation. The PO dosages for each compound were selected based on which had most clinical data available. For pravastatin, a 9.4 mg IV bolus dose and a 40 mg PO dose were examined; for rosuvastatin an 8 mg IV infusion and 80 mg PO dose were examined; for repaglinide a 2 mg IV infusion and 2 mg PO dose were examined; and for pitavastatin a 2 mg IV infusion and 2 mg PO dose were examined. Simulations were conducted for the base model, HEK293 buffer model, and HEK293 plasma model (Table 2).

Results

Uptake in OATP1B1- and OATB1B3-Overexpressing Cells

DMD Fast Forward. Published on May 6, 2021 as DOI: 10.1124/dmd.120.000315
This article has not been copyedited and formatted. The final version may differ from this version.

Details about the in vitro results and interpretation can be found in Bowman et al. (2020), and the data is presented here in Table 1. Briefly, differences for each parameter ($K_{m,u}$, J_{max}, and CL_{PD}) were found between the buffer and plasma incubations for both cells, with the largest differences noted for the highly protein bound repaglinide and pitavastatin. The $K_{m,u}$ values decreased in the plasma incubations as protein binding increased (with fold changes ranging from 1.91-619), while J_{max} values also decreased in the plasma as protein binding increased, but to a lesser extent than $K_{m,u}$ (the J_{max} fold changes ranged from 1.22-97.4). In addition, the CL_{PD} was higher in the human plasma incubations with the largest difference for pitavastatin (23.4 fold change) compared to the other three compounds (1.73-3.90 fold changes).

Transporter Quantitation

The full results of the transporter quantitation are presented in Supplementary Table 1. Ultimately the results from the ITPTDSR and NQTANLTNQGK peptides for OATP1B1 and OATP1B3 respectively were used for the calculation following Equation 1, leading to REF values of 5.63 for OATP1B1 and 1.87 for OATP1B3 as shown in Table 4.

PBPK Model Simulations

The simulated PK results can be found in Table 5 and Figures 1 and 2.

For pravastatin, the simulated PK parameters (the area under the concentration-time curve (AUC), the maximal concentration (C_{max}) and the time to the maximal concentration (t_{max})) fell within two-fold of the observed data for both the IV and oral doses using HEK293 data with REF in both plasma and buffer incubations (Table 5). The terminal phase of the IV profile was not fully captured with the HEK293 data, however given that it was not captured in the base

DMD Fast Forward. Published on May 6, 2021 as DOI: 10.1124/dmd.120.000315
This article has not been copyedited and formatted. The final version may differ from this version.

model, this is expected (Figure 1). The profiles of the oral dose were well-predicted (using both plasma and buffer incubation data) with the C_{max} and AUC predictions falling within the range of observed data. The sum of the OATP1B1 and OATP1B3 uptake $CL_{int,T}$ was relatively similar between the plasma (37.8 μL/min/10^6 cells), buffer (24.0 μL/min/10^6 cells), and base model (15.4 μL/min/10^6 cells). The use of a passive diffusion value from the HEK293 incubations vs. the SCHH of the base model was explored, and the simulation results were not affected (Supplementary Table 3). This was expected given the percentage of pravastatin entering the liver by passive diffusion was 1% or lower with all pravastatin data.

For rosuvastatin, the simulated PK parameters were also within two-fold of the observed data for both the IV and PO doses using the HEK293 data from both incubations (Table 5). The triphasic decline of the concentration-time profile of the IV dose appears to be better captured by the HEK293 plasma and buffer models (more of the observed data points fell within the 5^{th}/95^{th} percentile) than the base model (Figure 1). For the oral profile, the simulated C_{max} fell within the range of the observed, and the simulated AUC was slightly higher than the observed range using the HEK293 plasma and buffer models. In comparison, both the C_{max} and AUC were slightly underpredicted using the base model. These differences in simulations using the HEK293 models vs. the base model could be attributed to the difference in uptake $CL_{int,T}$ for OATP1B1 and OATP1B3—the sum of the uptake $CL_{int,T}$ for the two transporters in the HEK293 plasma incubations was 99.0 μL/min/10^6 cells, and for the HEK293 buffer incubations was 49.7 μL/min/10^6 cells; while it was much higher at 718 μL/min/10^6 cells for the base model. The percentage of rosuvastatin entering the liver by passive diffusion was less than 1% in all cases and using a passive diffusion value from the HEK293 cells vs. the SCHH of the base model yielded similar results (Supplementary Table 3).

DMD Fast Forward. Published on May 6, 2021 as DOI: 10.1124/dmd.120.000315
This article has not been copyedited and formatted. The final version may differ from this version.

With repaglinide, while the simulated PK parameters were within two-fold of the observed data for both the IV and oral doses using the HEK293 plasma and buffer models, there were differences in the predictions depending on the incubation data used. For the IV dose, the predicted AUC using the plasma model was 1.01-fold higher than the observed, while it was 1.85-fold higher with the buffer model. In addition, the concentration-time profile of the IV dose appeared to be better captured with the plasma model. Differences were also observed with the oral simulations. Using the plasma model the AUC, C_{max}, and concentration-time profile were slightly underpredicted, while using the buffer model, the AUC was predicted to be on the higher end of the observed values and the concentration-time profile was slightly overpredicted. In comparison to the base model with an OATP1B1 $CL_{int,T}$ of 838.1 μL/min/10^6 cells, the plasma model had a higher uptake of 1115 μL/min/10^6 cells, while the buffer model had a lower uptake of 225.7 μL/min/10^6 cells. The contribution of passive diffusion also varied and was higher than for the statins—the uptake percentage attributed to passive diffusion was 13.9% in the base model, was 2.8% with the plasma model, and was 7.4% with the buffer model. The lower contribution from the HEK293 cells provided more accurate predictions than the value from the SCHH of the base model (Supplementary Table 3).

Pitavastatin, the highest protein bound compound, had the largest difference between the in vitro kinetic parameters determined in HEK293 plasma vs. buffer incubations, and this held true for the PBPK simulation results as well. For the IV dose, the plasma model provided more accurate simulation results. The predicted AUC was within two-fold of the observed using the plasma model (1.4-fold underpredicted), and the shape of the concentration-time profile was closer to the observed (Table 5, Figure 1). The AUC was overpredicted using the buffer model by 4.4-fold and the concentration-time profile was not accurately captured. With the oral data,

DMD Fast Forward. Published on May 6, 2021 as DOI: 10.1124/dmd.120.000315
This article has not been copyedited and formatted. The final version may differ from this version.

the plasma model also provided more accurate simulations. The AUC and C_{max} were both underpredicted by 3-fold using the plasma model and this was closer to the observed data than using the buffer model. The AUC and C_{max} were overpredicted using the buffer model by 6.6-fold and 3.3-fold, respectively. In comparison, the base model (Duan et al. (2017)) used in vitro hepatocyte data and a scaling factor of 18 was required to achieve accurate predictions. More specifically, the optimized OATP1B1/3 $CL_{int,T}$ of Duan et al. (2017) was 1143 μL/min/10^6 cells, while the $CL_{int,T}$ of the plasma data was 3933 μL/min/10^6 cells without an empirical scaling factor and the $CL_{int,T}$ of the buffer data was 150.4 without an empirical scaling factor. The percentage of uptake by passive diffusion was less than 2% in all cases and similar results were seen using either the HEK293 cell or hepatocyte data (Supplementary Table 3).

Discussion

Generating transporter kinetic data from appropriate in vitro systems is crucial for accurate IVIVE and prediction of human PK profiles using PBPK modeling. While using hepatocytes has been explored, quantitatively using overexpressing cells and accounting for transporter expression is a more recent idea. This study explored the translational capability of data generated in transfected HEK293 cells with and without plasma and corrected for transporter expression, for human PK prediction using PBPK. To our knowledge, this is the first publication to demonstrate the bottom-up approach using in vitro OATP data directly without employing empirical scaling factors to predict the IV PK profiles reasonably well for multiple OATP substrates.

To understand the translation of OATP1B1/3 in vitro data, more emphasis was placed on capturing IV PK although both IV and PO simulations were conducted. Since alternative

DMD Fast Forward. Published on May 6, 2021 as DOI: 10.1124/dmd.120.000315
This article has not been copyedited and formatted. The final version may differ from this version.

transporters may contribute to the absorption of oral doses, accurately accounting for them is critical and any uncertainty would be independent of the OATP1B1/3 inputs explored here.

The expression levels of OATP1B1 and OATP1B3 in HEK293 overexpressing cells and human hepatocytes were determined using LC-MS/MS quantitation. The ITPTDSR and NQTANLTNQGK peptides for OATP1B1 and OATP1B3 respectively were selected due to the low interfering signal compared to control cells. In addition, they demonstrated good linearity for relative quantitation purposes during method qualification. Due to the complex nature of cellular extracts, all unique peptides detectable by LC-MS were quantitated. For IVIVE, choosing a peptide with the best intra-system selectivity and quantitative linearity is critical to accurate extrapolation.

Using theses REF values along with the previously reported J_{max} / $K_{m.}$values allowed exploration of bottom-up PBPK modeling of OATP contribution to compound PK. By investigating J_{max} / K_m values compared to the CL_{int} values of base models, potential saturation could also be taken into account. After scaling the in vitro data with REF, OATP1B1 had a larger contribution to the uptake than OATP1B3 for pravastatin, rosuvastatin, and pitavastatin. This highlights the value of using overexpressing cell lines to understand specific transporter contributions, and the larger contribution of OATP1B1 for these compounds aligns with previous in vitro (Kunze et al., 2014; Izumi et al., 2018) and in vivo pharmacogenomic (Yoshida et al., 2013) studies.

For the two compounds with lower protein binding, pravastatin and rosuvastatin, comparable transporter kinetics were generated in plasma and buffer incubations.. For pravastatin, the sum of the OATP1B1/3 uptake $CL_{int,T}$ was relatively similar between the plasma, buffer, and base models. For rosuvastatin, the OATP1B1/3 uptake $CL_{int,T}$ in the plasma and

DMD Fast Forward. Published on May 6, 2021 as DOI: 10.1124/dmd.120.000315
This article has not been copyedited and formatted. The final version may differ from this version.

buffer models were lower than the fitted OATP1B1/3 uptake CL_{int} of the base model, which agrees with the recent work of Kumar et al. (2020) who found that in vitro systems underpredicted rosuvastatin's uptake clearance, and suggested endogenous factors were missing. Despite this, the observed systemic clearance of rosuvastatin was still captured here and hepatic uptake may not be the rate-determining step (Billington et al., 2019). For the two highly protein bound compounds, repaglinide and pitavastatin, where the kinetic data were substantially different between the incubations, the OATP uptake $CL_{int,T}$ from the plasma incubations were more aligned with the fitted/optimized uptake $CL_{int,T}$ of the base models.

For the PBPK simulations of pravastatin and rosuvastatin, the pharmacokinetic parameters and concentration-time profiles of the IV doses were similar and overall well-predicted with the HEK293 plasma and buffer models. Larger differences in the repaglinide and pitavastatin simulations were noted, and the pharmacokinetic parameters and IV profiles were more accurately captured by the plasma models than the buffer models for both. While pitavastatin's concentration-time profile was not fully captured, this may be because the current base model does not include enterohepatic recirculation and/or because the volume is underpredicted (Kojima et al., 2001; Catapano, 2012).

It should be noted that the half-lives of pravastatin and pitavastatin were not accurately reflected in the base models (Supplementary Table 4). This manuscript shows promise for prospective predictions of clearance, which contribute to successful half-life predictions. On the other side, it is important to mention the gap that current volume predictions do not incorporate the impact of transporters, which may lead to higher observed values (Grover and Benet, 2009). Since the Rodgers and Rowland (2007) prediction method used does not account for transporters, it was not surprising to see half-life prediction error given the dependency on both clearance and

DMD Fast Forward. Published on May 6, 2021 as DOI: 10.1124/dmd.120.000315
This article has not been copyedited and formatted. The final version may differ from this version.

volume. As an exercise, the Vss was retrospectively raised to the observed range by increasing the Kp scalar, which improved half-life predictions, did not largely impact CL predictions (Supplementary Table 4) and slightly improved PK profile predictions (Supplementary Figure 1). While it was beyond the scope of this work to improve the bottom-up approach for volume predictions, using allometry or tissue concentration data from rats (Chan et al., 2019) could be explored.

The results presented here align with previous work examining the hypothesis of protein-facilitated uptake (Baik and Huang, 2015; Fukuchi et al., 2017; Bowman et al., 2019; Bteich et al., 2019; Kim et al., 2019; Bi et al., 2020; Francis et al., 2020; Liang et al., 2020; Li et al., 2021). According to this idea, interactions between the drug-protein complex and the hepatocyte cell surface or transporters may lead to greater uptake and clearance for highly protein bound drugs (primarily acidic drugs examined to date) than would be predicted using traditional in vitro methods with protein-free buffer. The PBPK modeling results for repaglinide and pitavastatin emphasize that there is a difference when using in vitro data generated with and without plasma, and suggest that plasma data may reflect the physiologically relevant condition, as the simulations for the highly bound OATP substrates captured the observed PK more closely than those using protein-free buffer data. Alternative explanations could be that plasma reduces the non-specific incubation binding and/or improves the solubility of compounds, and more work is needed to mechanistically understand the differences seen between plasma vs. protein-free buffer.

Ultimately the in vitro underprediction of clearance is likely multifactorial (Bowman and Benet, 2016; Wood et al., 2017), however, the inclusion of REF and the kinetic parameters presented here bring hope for the traditionally difficult bottom-up modeling of OATP substrates.

DMD Fast Forward. Published on May 6, 2021 as DOI: 10.1124/dmd.120.000315
This article has not been copyedited and formatted. The final version may differ from this version.

The base models of the four compounds either used fitted clinical data to obtain a global $CL_{int,T}$ (and assigned fractions transported from in vitro data) (Jamei et al., 2014; Simcyp 2019; Simcyp 2020), or used SCHH data and required an 18-fold empirical scaling factor (Duan et al., 2017). Supplementary Table 5 describes the OATP1B1/3 inputs from additional models developed in the Simcyp simulator beyond those used here. For pravastatin, Varma et al. (2012) found that SCHH data overpredicted the IV concentration-time profile, leading to a scaling factor of 31; while Mao et al. (2018) found that plateable human hepatocytes in plasma could accurately capture pravastatin's disposition. For rosuvastatin, Emami Riedmaier et al. (2016) and Wang et al. (2017) input a fitted global uptake $CL_{int,T}$ from clinical data, and assigned transporter contributions from in vitro data. For repaglinide, Varma et al. (2012) used SCHH data and needed a 17-fold empirical scaling factor. Additionally, Jones et al. (2012) input SCHH data for PBPK modeling using Berkeley Madonna and determined scaling factors of 21 for pravastatin, 12 for rosuvastatin, and 44 for repaglinide were needed to capture the active uptake in their models.

Based on the results presented here, selecting a physiologically relevant in vitro system such as HEK293 overexpressing cells (with or without plasma for low protein binding OATP substrates, and with plasma for high protein binding OATP substrates) and incorporating transporter quantitation may help achieve more accurate prospective PK predictions. This work demonstrates that the approach may avoid the compound-specific empirical scaling factors previously needed. For pravastatin and rosuvastatin, predictions may have been more accurate than previous work if there were functional activity differences with the transporters in the HEK293 cells and the previously used hepatocytes. Having accurate REF values may have also improved predictability: the transporter abundances were measured using the same experimental

DMD Fast Forward. Published on May 6, 2021 as DOI: 10.1124/dmd.120.000315
This article has not been copyedited and formatted. The final version may differ from this version.

procedures for HEK293 cells and hepatocytes in-house; the same HEK293 lots used for kinetic data were used for abundance measurements; and a 10-donor mixed gender pooled hepatocyte lot was used to avoid interindividual variability. For repaglinide and pitavastatin, predictions may have been more accurate for the same reasons in addition to the use of plasma incubations. Although passive diffusion was a relatively small percentage of the uptake of these compounds, differences between plasma vs. buffer incubations should be further explored and could impact predictions of compounds with larger passive contributions. Differences in passive diffusion between incubations have been noted with hepatocytes as well (Bowman et al., 2019; Liang et al., 2020), and possible explanations have been methodological or physiological (Liang et al., 2020).

In conclusion, using HEK293 overexpressing transporter cells in plasma incubations and accounting for transporter expression demonstrates a promising approach for bottom-up PBPK modeling of OATP substrates. As additional hypotheses for the in vitro to in vivo discrepancy of transporter substrates are examined, such as differences with endogenous factors in vitro/in vivo, they could be built into this in vitro system and modeling approach.

DMD Fast Forward. Published on May 6, 2021 as DOI: 10.1124/dmd.120.000315
This article has not been copyedited and formatted. The final version may differ from this version.

Acknowledgements

The authors would like to thank Robert S. Jones for the hepatocyte protein measurement; Matthew Harwood and Sibylle Neuhoff from Certara for their discussions; and Eugene Chen and Kenta Yoshida for their review.

Participated in research design: Bowman, B. Chen, Cheong, Liu, Y, Chen, Mao.
Conducted experiments: Bowman, B. Chen, Cheong, Liu.
Contributed new reagents or analytic tools: B. Chen, Cheong, Liu.
Performed data analysis: Bowman, B. Chen, Cheong, Liu, Y, Chen, Mao.
Wrote or contributed to the writing of the manuscript: Bowman, B. Chen, Cheong, Liu, Y, Chen, Mao.

DMD Fast Forward. Published on May 6, 2021 as DOI: 10.1124/dmd.120.000315
This article has not been copyedited and formatted. The final version may differ from this version.

References

Aberg JA, Rosenkranz SL, Fichtenbaum CJ, Alston BL, Brobst SW, Segal Y and Gerber JG (2006) Pharmacokinetic interaction between nelfinavir and pravastatin in HIV-seronegative volunteers: ACTG study A5108. *AIDS*. **20:**725-729.

Backman JT, Kyrklund MB, Neuvonen M and Neuvonen PJ (2002) Gemfibrozil greatly increases plasma concentrations of cerivastatin. *Clin Pharmacol Ther*. **72:**685-691.

Baik J and Huang Y (2015) Transporter-induced protein binding shift (TIPBS) hypothesis and modeling, in 20th North American ISSX Meeting. Orlando, Florida, October 2015.

Bi Y, Ryu S, Tess DA, Rodrigues D and Varma MVS (2020) Effect of human plasma on hepatic uptake of organic anion-transporting polypeptide 1B substrates: studies using transfected cells and primary human hepatocytes. *Drug Metab Dispos.* DOI: https://doi.org/10.1124/dmd.120.000134

Bidstrup TB, Bjornsdottir I, Sidelmann UG, Thomsen MS and Hansen KT (2003) CYP2C8 and CYP3A4 are the principal enzymes involved in the human in vitro biotransformation of the insulin secretagogue repaglinide. *Br J Clin Pharmacol*. **56:**305-314.

Billington S, Shoner S, Lee S, Clark-Snustad K, Pennington M, Lewis D et al. (2019) Positron emission tomography imaging of [^{11}C]rosuvastatin hepatic concentrations and hepatobiliary transport in humans in the absence and presence of cyclosporin A. *Clin. Pharmacol. Ther.* **106**:1056-1066.

Bosgra S, van de Steeg E, Vlaming ML, Verhoeckx KC, Huisman MT, Verwei M, and Wortelboer HM (2014) Predicting carrier-mediated hepatic disposition of rosuvastatin in man by scaling from individual transfected cell-lines in vitro using absolute transporter protein quantification and PBPK modeling. *Eur J Pharm Sci.* **65:**156-166.

Bowman CM and Benet LZ (2016) Hepatic clearance predictions from in vitro-in vivo extrapolation and the biopharmacetuics drug disposition classification system. *Drug Metab Dispos.* **44:**1731-1735.

Bowman CM, Chen E, Chen L, Chen YC, Liang X, Wright M, Chen Y and Mao J (2020) Changes in organic anion transporting polypeptide uptake in HEK293 overexpressing cells in the presence and absence of human plasma. *Drug Metab Dispos*. **48:**18-24.

Bowman CM, Okochi H, and Benet LZ (2019) The presence of a transporter-induced protein binding shift: a new explanation for protein-facilitated uptake and improvement for in vitro-in vivo extrapolation. *Drug Metab Dispos*. **47:**358-363.

Bowman CM, Ma F, Mao J and Chen Y (2020) Examination of physiologically-based pharmacokinetic (PBPK) models of rosuvastatin. *Accepted in CPT:PSP*.

Bteich M, Poulin P, and Haddad S (2019) The potential protein-mediated hepatic uptake: discussion on the molecular interactions between albumin and the hepatocyte cell surface and their implications for the in vitro-to-in vivo extrapolations of hepatic clearance of drugs. *Expert Opin Drug Metab Toxicol*. **15:**633-658.

Burt HJ, Emami Riedmaier A, Harwood MD, Kim Crewe H, Gill KL and Neuhoff S (2016) Abundance of hepatic transporters in caucasians: a meta-analysis. *Drug Metab. Dispos.* **44**:1550-1561.

Catapano AL (2012) Pitavastatin: a different pharmacological profile. *Clinical Lipidology*. **7:**sup1, 3-9

Chan JCY, Tan SPF, Upton Z, and Chan ECY (2019) Bottom-up physiologically-based biokinetic modelling as an alternative to animal testing. *ALTEX*. **36**: 597-612.

Cooper KJ, Martin PD, Dane AL, Warwick MJ, Schneck DW and Cantarini MV (2002) The effect of fluconazole on the pharmacokinetics of rosuvastatin. *Eur J Clin Pharmacol*. **58**:527-531.

Cooper KJ, Martin PK, Dane AL, Warwick MJ, Schneck DW and Cantarini MV (2003a) Effect of itraconazole on the pharmacokinetics of rosuvastatin. *Clin Pharmacol Ther*. **73**:322-329.

Cooper KJ, Martin PD, Dane AL, Warwick MJ, Raza A and Schneck DW (2003b) The effect of erythromycin on the pharmacokinetics of rosuvastatin. *Eur J Clin Pharmacol*. **59**:51-56.

Duan, P., Zhao, Pi and Zhang L (2017) Physiologically-based pharmacokinetic (PBPK) modeling of pitavastatin and atorvastatin to predict drug-drug interactions (DDIs). *Eur J Drug Metab Pharmacokinet*. **42**:689-705.

Emami Riedmaier A, Burt H, Abduljalil K and Neuhoff S (2016) More power to OATP1B1: an evaluation of sample size in pharmacogenetic studies using a rosuvastatin PBPK model for intestinal, hepatic, and renal transporter-mediated clearance. *J Clin Pharmacol*. **56**:S132-142.

FDA. Pitavastatin Clinical Pharmacology and Biopharmaceutics Review. https://www.accessdata.fda.gov/drugsatfda_docs/nda/2009/022363s000TOC.cfm Accessed April 2021.

Francis LJ, Houston B and Hallifax D (2020) Impact of plasma protein binding in drug clearance prediction: a database analysis of published studies and implications for in vitro in vivo extrapolation. *Drug Metab Dispos*. DOI: https://doi.org/10.1124/dmd.120.000294

Fukuchi Y, Toshimoto K, Mori T, Kakimoto K, Tobe Y, Sawada T et al. (2017) Analysis of nonlinear pharmacokinetics of a highly albumin-bound compound: contribution of albumin-mediated hepatic uptake mechanism. *J. Pharm. Sci.* **106**:2704-2714.

Giacomini KM, Huang SM, Tweedie DJ, Benet LZ, Brouwer KL, Chu X, Dahlin A, Evers R, Fischer V, Hillgren KM, Hoffmaster KA, Ishikawa T, Keppler D, Kim RB, Lee CA, Niemi M, Polli JW, Sugiyama Y, Swaan PW, Ware JA, Wright SH, Yee SW, Zamek-Gliszczynski MJ, and Zhang, L (2010) Membrane transporters in drug development. *Nat Rev Drug Discov* **9:**215-236.

Grimstein M, Yang Y, Zhang X, Grillo J, Huang S-M, Zineh I and Wang Y (2019) Physiologically Based Pharmacokinetic Modeling in Regulatory Science: an update from the U.S. Food and Drug Administration's Office of Clinical Pharmacology. *J Pharm Sci*. **108:**21-25.

Harwood et al., Manuscript in preparation.

Hatorp V, Oliver S and Su CA (1998) Bioavailability of repaglinide, a novel antidiabetic agent, administered orally in tablet or solution form or intravenously in healthy male volunteers. *Int J Clin Pharmacol Ther*. **36:**636-641.

Hatorp V, Huang WC and Strange P (1999) Repaglinide pharmacokinetics in healthy young adult and elderly subjects. *Clin Ther*. **21:**702-710.

Hatorp V, Hansen KT and Thomsen MS (2003) Influence of drugs interacting with CYP3A4 on the pharmacokinetics, pharmacodynamics, and safety of the prandial glucose regulator repaglinide. *J Clin Pharmacol*. **43:**649-660.

Hirano M, Maeda K, Shitara Y and Sugiyama Y (2004) Contribution of OATP2 (OATP1B1) and OATP8 (OATP1B3) to the hepatic uptake of pitavastatin in humans. *J Pharmacol Exp Ther*. **311**:139-146.

Hirano M, Maeda K, Matsushima S, Nozaki Y, Kusuhara H and Sugiyama Y (2005) Involvement of BCRP (ABCG2) in the biliary excretion of pitavastatin. *Mol Pharmacol.* **68:**800-807.

Hirano M, Maeda K, Shitara Y and Sugiyama Y (2006) Drug-drug interaction between pitavastatin and various drugs via OATP1B1. *Drug Metabol Dispos Biol Fate Chem*. **34:**1229-1236.

Ishida K, Ullah M, Toth B, Juhasz V, and Unadkat J (2018) Successful prediction of in vivo hepatobiliary clearances and hepatic concentrations of rosuvastatin using sandwich-cultured rat hepatocytes, transporter-expressing cell lines, and quantitative proteomics. *Drug Metab Dispos*. **46:**66-74.

Izumi S, Nozaki Y, Komori T, Takenaka O, Maeda K, Kusuhara H and Sugiyama Y (2017) Comparison of the predictability of human hepatic clearance for organic anion transporting polypeptide substrate drugs between different in vitro-in vivo extrapolation approaches. *J. Pharm. Sci.* **106**:2678-2687.

Izumi S, Nozaki Y, Kusuhara H, Hotta K, Mochizuki T, Komori T et al. (2018) Relative activity factor (RAF)-based scaling of uptake clearance mediated by organic anion transporting

polypeptide (OATP) 1B1 and OATP1B3 in human hepatocytes. *Mol. Pharmaceutics.* **15**:2277-2288.

Jamei M, Bajot F, Neuhoff S, Barter Z, Yang J, Rostami-Hodjegan A and Rowland-Yeo K (2014) A mechanistic framework for in vitro-in vivo extrapolation of liver membrane transporters: prediction of drug-drug interaction between rosuvastatin and cyclosporine. *Clin Pharmacokinet*. **53:**73-87.

Jamei M, Turner D, Yang J, Neuhoff S, Polak S, Rostami-Hodjegan A and Tucker G (2009) Population-based mechanistic prediction of oral drug absorption. *AAPS J*. **11**:225-237.

Jones HM, Barton HA, Lai Y, Bi YA, Kimoto E, Kempshall S, Tate SC, El-Kattan A, Houston JB, Galetin A and Fenner KS (2012) Mechanistic pharmacokinetic modeling for the prediction of transporter-mediated disposition in humans from sandwich culture human hepatocyte data. *Drug Metab Dispos*. **40:**1007-1017.

Kajosaari LI, Niemi M, Neuvonen M, Latila J, Neuvonen PJ and Backman JT (2005) Cyclosporine markedly raises the plasma concentrations of repaglinide. *Clin Pharmacol Ther*. **78**:388-399.

Kantola T, Backman JT, Niemi M, Kivisto KT and Neuvonen PJ (2000) Effect of fluvonazole on plasma fluvastatin and pravastatin concentrations. *Eur J Clin Pharmacol*. **56:**225-229.

Kim S-J, Lee K-R, Miyauchi S and Sugiyama Y (2019) Extrapolation of in vivo hepatic clearance from in vitro uptake clearance by suspended human hepatocytes for anionic drugs with high binding to human albumin: improvement of in vitro-to-in vivo extrapolation by considering the "albumin-mediated" hepatic uptake mechanism on the basis of the "facilitated-dissociation model". *Drug Metab Dispos* **47:**94-103.

Kojima J, Ohshima T, Yoneda M and Sawada H (2001) Effect of biliary excretion on the pharmacokinetics of pitavastatin (NK-104) in dogs. *Xenobio. Metabol. And Dispos.* **16:**497-502.

Kyrklund C, Backman JT, Neuvonen M, Neuvonen PJ (2003) Gemfibrozil increases plasma pravastatin concentrations and reduces pravastatin renal clearance. *Clin Pharmacol Ther*. **73**:538-544.

Kunze A, Huwyler J, Camenisch G and Poller B (2014) Prediction of organic anion-transporting polypeptide 1B1- and 1B3-mediated hepatic uptake of statins based on transporter expression and activity data. *Drug Metab. Dispos.* **42**:1514-1521.

Kumar V, Yin M, Ishida K, Salphati L, Hop CECA, Rowbottom C et al. (2020) Prediction of transporter-mediated rosuvastatin hepatic uptake clearance and drug interaction in humans using proteomics-informed REF approach. *Drug Metab Dispos*. DOI: https://doi.org/10.1124/dmd.120.000204

Li N, Bi YA, Duignan DB and Lai Y (2009) Quantitative expression profile of hepatobiliary transporters in sandwich cultured rat and human hepatocytes. *Mol Pharm.* **6**:1180-1189.

Li R, Barton HA and Varma MV (2014) Prediction of pharmacokinetics and drug-drug interactions when hepatic transporters are involved. *Clin Pharmacokinet*. **53:**659-678.

Li N et al. (2021) Albumin-mediated uptake improves human clearance prediction for hepatic uptake transporter substrates aiding a mechanistic in vitro-in vivo extrapolation (IVIVE) strategy in discovery research. *AAPS J*. **23**:1 doi: 10.1208/s12248-020-00528-y

Liang X, Park Y, DeForest N, Hao J, Zhao X, Miu C et al. (2020) In vitro hepatic uptake in human and monkey hepatocytes in the presence and absence of serum protein and its in vitro to in vivo extrapolation. *Drug Metab Dispos*. DOI: 10.1124/dmd.120.000163

Mao J, Doshi U, Wright M, Hop CECA, Li AP and Chen Y (2018) Prediction of the pharmacokinetics of pravastatin as an OATP substrate using plateable human hepatocytes with human plasma data and PBPK modeling. *CPT Pharmacometrics Syst Pharmacol*. **7:**251-258.

Martin PD, Warwick, MJ, Dane AL, Brindley C, and Short T (2003a) Absolute oral bioavailability of rosuvastatin in healthy white adult male volunteers. *Clin Ther*. **25**:2553-2563.

Martin PD, Warwick MJ, Dane AL and Cantarini MV (2003b) A double-bind, randomized, incomplete crossover trial to assess the dose proportionality of rosuvastatin in healthy volunteers. *Clin Ther*. **25**:2215-2224.

Neuhoff, S and Tucker, GT (2013) Comment on the article "physiologically based modeling of pravastatin transporter-mediated hepatobiliary disposition and drug-drug interactions". *Pharm Res.* **30**:1467–1468

Neuvonen PJ, Kantola T and Kivisto KT (1998) Simvastatin but not pravastatin is very susceptible to interaction with the CYP3A4 inhibitor itraconazole. *Clin Pharmacol Ther*. **63:**332-341.

Niemi M et al. (2005) Polymorphic organic anion transporting polypeptide 1B1 is a major determinant of repaglinide pharmacokinetics. *Clin Pharmacol Ther*. **77**:468-478.

Pasanen MK, Fredrikson H, Neuvonen PJ and Niemi M (2007) Different effects of SLCO1B1 polymorphism on the pharmacokinetics of atorvastatin and rosuvastatin. *Clin Pharmacol Ther*. **82:**726-733.

Pfeifer N, Yang K and Brouwer, KLR (2013) Hepatic basolateral efflux contributes significantly to rosuvastatin disposition I: characterization of basolateral versus biliary clearance using a novel protocol in sandwich-cultured hepatocytes. *J. Pharmacol. Exp. Ther*. **347**:727-736.

Rodgers T and Rowland M (2007) Mechanistic approaches to volume of distribution predictions: understanding the processes. *Pharm Res*. **24**:918-933.

Rostami-Hodjegan, A. (2012) Physiologically based pharmacokinetics joined with in vitro-in vivo extrapolation of ADME: a marriage under the arch of systems pharmacology. *Clin. Pharmacol. Ther*. **92:**50-61.

Sager JE, Yu J, Ragueneau-Majlessi I and Isoherranen N (2015) Physiologically based pharmacokinetic (PBPK) modeling and simulation approaches: a systematic review of published models, applications, and model verification. *Drug Metab Dispos*. **41**:1823-1837.

Schneck DW, Birmingham BK, Zalikowski JA, Mitchell PD, Wang Y, Martin PK, Lasseter KC, Brown CD, Windass AS and Raza A (2004) The effect of gemfibrozil on the pharmacokinetics of rosuvastatin. *Clin Pharmacol Ther*. **75**:455-463.

Shitara, Y (2011) Clinical importance of OATP1B1 and OATP1B3 in drug-drug interactions. *Drug Metab Pharmacokinet.* **26**:220-227.

Simcyp. Repaglinide compound file summary (2019).

Simcyp. Pravastatin compound file summary (2020).

Simonson SG, Raza A, Martin PD, Mitchell PD, Jarcho JA, Brown CDA, Windass AS and Schneck DW (2004) Rosuvastatin pharmacokinetics in heart transplant recipients administered an antirejection regimen including cyclosporine. *Clin Pharmacol Ther*. **76**:167-177.

Singhvi SM, Pan HY, Morrison RA and Willard DA (1990) Disposition of pravastatin sodium, a tissue-selective HMG-CoA reductase inhibitor, in healthy subjects. *Br J Clin Pharmacol*. **29:**239-243.

Taskar K, Reddy VP, Burt H, Posada MM, Varma M, Zheng M et al. (2019) PBPK models for evaluating membrane transporter mediated DDIs: current capabilities, case studies, future opportunities and recommendations. *Clin Pharmacol Ther*. **107:**1082-1115.

Varma MVS, Lai Y, Feng B, Litchfield J, Goosen TC and Bergman A (2012) Physiologically based modeling of pravastatin transporter-mediated hepatobiliary disposition and drug-drug interactions. *Pharm Res*. **29:**2860-2873.

Varma MVS, Lai Y, Kimoto E, Goosen TC, El-Kattan AF and Kumar V (2013) Mechanistic modeling to predict the transporter- and enzyme-mediated drug-drug interactions of repaglinide. *Pharm Res*. **30:**1188-1199.

Wang Q, Zheng M and Leil T (2017) Investigating transporter-mediated drug-drug interactions using a physiologically based pharmacokinetic model of rosuvastatin. *CPT Pharmacometrics Syst Pharmacol.* **6**:228-238.

Wood FL, Houston JB and Hallifax D (2017) Clearance prediction methodology needs fundamental improvement: trends common to rat and human hepatocytes/microsomes and implications for experimental methodology. *Drug Metab Dispos.* **45**:1178-1188.

Yoshida K, Maeda K and Sugiyama Y (2013) Hepatic and intestinal drug transporters: prediction of pharmacokinetic effects caused by drug-drug interactions and genetic polymorphisms. *Annu. Rev. Pharmacol. Toxicol.* **53**:581-612.

Zhang W et al. (2006) Efffect of SLCO1B1 genetic polymorphism on the pharmacokinetics of nateglinide. *Br J Clin Pharmacol*. **62**:567-572.

DMD Fast Forward. Published on May 6, 2021 as DOI: 10.1124/dmd.120.000315
This article has not been copyedited and formatted. The final version may differ from this version.

Footnote

This work was supported by Genentech, and received no external funding.

DMD Fast Forward. Published on May 6, 2021 as DOI: 10.1124/dmd.120.000315
This article has not been copyedited and formatted. The final version may differ from this version.

Figure Legends

Figure 1: Simulated IV and PO concentration-time profiles of pravastatin, rosuvastatin, repaglinide, and pitavastatin using base models, HEK293 buffer models, and HEK293 plasma models. The simulated results are shown as a green line with the 5^{th} and 95^{th} percentiles shown as grey lines. The observed clinical data (references can be found in Table 3) are plotted as points.

Figure 2: Comparison of the AUC observed vs. AUC predicted for the IV doses of pravastatin, rosuvastatin, repaglinide, and pitavastatin using the HEK293 plasma and HEK293 buffer models. The x-axis shows the observed AUC reported in the references of Table 3, and the y-axis shows the predicted AUC from the plasma and buffer models.

DMD Fast Forward. Published on May 6, 2021 as DOI: 10.1124/dmd.120.000315
This article has not been copyedited and formatted. The final version may differ from this version.

Table 1: The J_{max}, $K_{m,u}$, and CL_{PD} values previously generated for pravastatin, rosuvastatin, repaglinide, and pitavastatin in OATP1B1 and OATP1B3 overexpressing cells in human plasma and buffer (Bowman et al., 2020).

		OATP1B1 J_{max} / $K_{m,u}$ (pmol/min/mg / μM)	**OATP1B3** J_{max} / $K_{m,u}$ (pmol/min/mg / μM)	CL_{PD} (uL/min/mg protein)
Pravastatin	**Plasma**	224 / 44.5	145 / 28.5	0.614
	Buffer	274 / 84.9	179 / 57.5	0.159
Rosuvastatin	**Plasma**	50.0 / 3.25	37.1 / 5.61	2.64
	Buffer	132 / 22.2	156 / 18.0	0.677
Repaglinide	**Plasma**	1.98 / 0.0100	-	84.2
	Buffer	42.9 / 1.07	-	48.6
Pitavastatin	**Plasma**	5.69 / 0.00855	1.56 / 0.0157	148
	Buffer	111 / 5.29	152 / 8.80	6.33

DMD Fast Forward. Published on May 6, 2021 as DOI: 10.1124/dmd.120.000315
This article has not been copyedited and formatted. The final version may differ from this version.

Table 2: Summary of the key input parameters of pravastatin, rosuvastatin, repaglinide, and pitavastatin used in the base model, HEK293 plasma model and HEK293 buffer model.

		Pravastatin	**Rosuvastatin**	**Repaglinide**	**Pitavastatin**
	Physicochemical Properties				
	MW	424.53	481.54	452.6	421.46
	LogP	2.2	2.4	5.18	2.91
	Compound Type	Monoprotic Acid	Monoprotic Acid	Ampholyte	Monoprotic Acid
	pKa	4.55	4.27	4.18, 6.02	5.31
	Fraction Unbound	0.485	0.107	0.0188	0.005
	Blood/Plasma Ratio	0.556	0.625	0.566	0.55
	Absorption				
	Model	ADAM	ADAM	First-Order Absorption	ADAM
	Distribution				
	Model	Full PBPK	Full PBPK	Full PBPK	Full PBPK
	Elimination				
	Metabolism	HLM CL_{int}	HLM CL_{int}	CYP3A4, CYP2C8	CYP2C8, CYP2C9, UGT, HLM CL_{int}
	CL_R (L/hr)	Permeability-limited model	In vivo data	In vivo data	In vivo data
	Transport				
	Liver				
Base Model	CL_{PD} (ml/min/10^6 cells)	0.000109	0.00136	0.089	0.011
	OATP1B1 $CL_{int,T}$ (uL/min/10^6 cells)	14.057	597	838.11	58.4
	RAF/REF	1	1		18
	OATP1B3 $CL_{int,T}$ (uL/min/10^6 cells)	1.343	121		5.1
	RAF/REF	1	1		18
HEK293 Plasma Model	CL_{PD} (ml/min/10^6 cells)	0.000147	0.000632	0.0201	0.0354
	OATP1B1 J_{max} / $K_{m,u}$ (pmol/min/mg / μM)	224 / 44.5	50.0 / 3.25	1.98 / 0.0100	5.69 / 0.00855
	REF (mg/10^6 cells)	5.63	5.63	5.63	5.63
	OATP1B3 J_{max} / $K_{m,u}$ (pmol/min/mg / μM)	145 / 28.5	37.1 / 5.61	-	1.56 / 0.0157
	REF (mg/10^6 cells)	1.87	1.87	-	1.87
HEK293 Buffer Model	CL_{PD} (ml/min/10^6 cells)	0.0000380	0.000162	0.0116	0.00151
	OATP1B1 J_{max} / $K_{m,u}$ (pmol/min/mg / μM)	274 / 84.9	132 / 22.2	42.9 / 1.07	111 / 5.29

DMD Fast Forward. Published on May 6, 2021 as DOI: 10.1124/dmd.120.000315
This article has not been copyedited and formatted. The final version may differ from this version.

	REF (mg/10^6 cells)	5.63	5.63	5.63	5.63
	OATP1B3 J_{max} / $K_{m,u}$ (pmol/min/mg / μM)	179 / 57.5	156 / 18.0	-	152 / 8.80
	REF (mg/10^6 cells)	1.87	1.87	-	1.87
	Additional Transporters	MRP2 (intestine, liver), OAT3 (kidney), MATE (kidney)	OATP2B1 (intestine, liver), NTCP (liver), BCRP (liver), MRP4 (liver)		

HEK293 $CL_{int,T}$ (uL/min/10^6 cells) = (J_{max} (pmol/min/mg)/ $K_{m,u}$ (uM)) * REF (mg/10^6 cells)

DMD Fast Forward. Published on May 6, 2021 as DOI: 10.1124/dmd.120.000315
This article has not been copyedited and formatted. The final version may differ from this version.

Table 3: Pharmacokinetic studies of pravastatin, rosuvastatin, repaglinide, and pitavastatin examined for this analysis and the simulations run using the Simcyp simulator.

	Number of Subjects	Age (years)	Proportion of Females	Reference
Pravastatin IV (9.4 mg, bolus)				
	8	21-39	N.R.	Singhvi et al. (1990)
Simcyp Simulation	**8**	**21-39**	**0.50**	
Pravastatin PO (40 mg)				
	10	19-23	0.30	Neuvonen et al. (1998)
	12	19-26	0.75	Kantola et al. (2000)
	14	N.R.	0.50	Aberg et al. (2006)
Simcyp Simulation	**36**	**19-26**	**0.53**	
Rosuvastatin IV (8 mg, infusion)				
	10	21-51	0	Martin et al. (2003a)
Simcyp Simulation	**10**	**21-51**	**0**	
Rosuvastatin PO (80 mg)				
	14	25-56	0	Cooper et al. (2003a)
	11	22-44	0	Cooper et al. (2003b)
	14	29-51	0	Cooper et al. (2002)
	18	31-60	0	Martin et al. (2003b)
	20	35-47	0.15	Schneck et al. (2004)
Simcyp Simulation	**77**	**22-60**	**0.039**	
Repaglinide IV (2 mg, infusion)				
	12	18 – 45	0.0	Hatorp et al. (1998)
Simcyp Simulation	**12**	**18 – 45**	**0.0**	
Repaglinide PO (2 mg)				

DMD Fast Forward. Published on May 6, 2021 as DOI: 10.1124/dmd.120.000315
This article has not been copyedited and formatted. The final version may differ from this version.

	24	18 – 49	0.0	Hatorp et al. (1998)
	12	18 – 40	0.5	Hatorp et al. (1999)
	8	18 – 45	0.0	Hatorp et al. (2003)
	16	18 – 45	0.375	Hatorp et al. (2003)
	11	18 – 45	1.0	Hatorp et al. (2003)
	12	18 – 45	0.0	Hatorp et al. (2003)
Simcyp Simulation	**83**	**18 – 49**	**0.277**	
Pitavastatin IV (2 mg, infusion)				
	18	N.R.	0.0	FDA
Simcyp Simulation	**18**	**21-51**	**0.0**	
Pitavastatin PO (2 mg)				
	18	N.R.	0.0	FDA
Simcyp Simulation	**18**	**21-51**	**0.0**	

*N.R.= not reported

DMD Fast Forward. Published on May 6, 2021 as DOI: 10.1124/dmd.120.000315
This article has not been copyedited and formatted. The final version may differ from this version.

Table 4: Calculation of REF values used for OATP1B1 and OATP1B3.

	HEK293 Overexpressing Cells (pmol/mg protein)	**Hepatocytes (pmol/10^6 cells)**	**HEK293 Overexpressing Cells (mg protein/10^6 cells)**	**Hepatocytes (mg protein/10^6 cells)**	**REF**
OATP1B1	1.51	6.91	0.239	0.294	5.63
OATP1B3	0.672	1.02	0.238	0.294	1.87

DMD Fast Forward. Published on May 6, 2021 as DOI: 10.1124/dmd.120.000315
This article has not been copyedited and formatted. The final version may differ from this version.

Table 5: The geometric mean (AUC, C_{max}) and median (t_{max}) of the observed and simulated PK parameters for pravastatin, rosuvastatin, repaglinide, and pitavastatin. The ratio (observed/predicted) is in parentheses.

Compound	Data	IV	PO		
		AUC (ng *hr/mL)	AUC (ng*hr/mL)	C_{max} (ng/mL)	t_{max} (hr)
Pravastatin	Observed	171.2	86.5 – 111	27.9 – 49.5	1.2 – 1.7
	Base Model	176.1 (0.97)	199 (0.43 – 0.56)	67.9 (0.41 – 0.73)	0.97
	HEK293 plasma	147.1 (1.16)	95.9 (0.90 – 1.16)	33.4 (0.84 – 1.48)	0.93
	HEK293 buffer	157.8 (1.08)	133 (0.65 – 0.83)	46.1 (0.61 – 1.07)	0.94
Rosuvastatin	Observed	164	253 – 410	30.1 – 53.5	3.0 – 5.0
	Base Model	157.5 (1.04)	197 (1.28 – 2.08)	17.4 (1.73 – 3.07)	3.10
	HEK293 plasma	197.8 (0.83)	412 (0.61 – 1.00)	36.3 (0.83 – 1.47)	3.23
	HEK293 buffer	205.7 (0.80)	454 (0.56 – 0.90)	40.0 (0.75 - 1.34)	3.26
Repaglinide	Observed	61.4	27.2 – 69.0	20.2 – 47.9	0.50 – 0.90
	Base Model	86.2 (0.71)	36.9 (0.74 – 1.87)	26.5 (0.76 – 1.81)	0.57
	HEK293 plasma	61.7 (1.00)	16.3 (1.67 – 4.23)	14.2 (1.42 – 3.37)	0.48
	HEK293 buffer	113.6 (0.54)	61.7 (0.44 – 1.12)	38.4 (0.53 – 1.25)	0.60
Pitavastatin	Observed	76.1	33.6	18.6	0.75
	Base Model	87.6 (0.87)	33.8 (0.99)	18.3 (1.02)	0.79
	HEK293 plasma	55.4 (1.37)	10.4 (3.23)	6.54 (2.84)	0.69
	HEK293 buffer	334 (0.23)	221 (0.15)	62.0 (0.30)	1.09

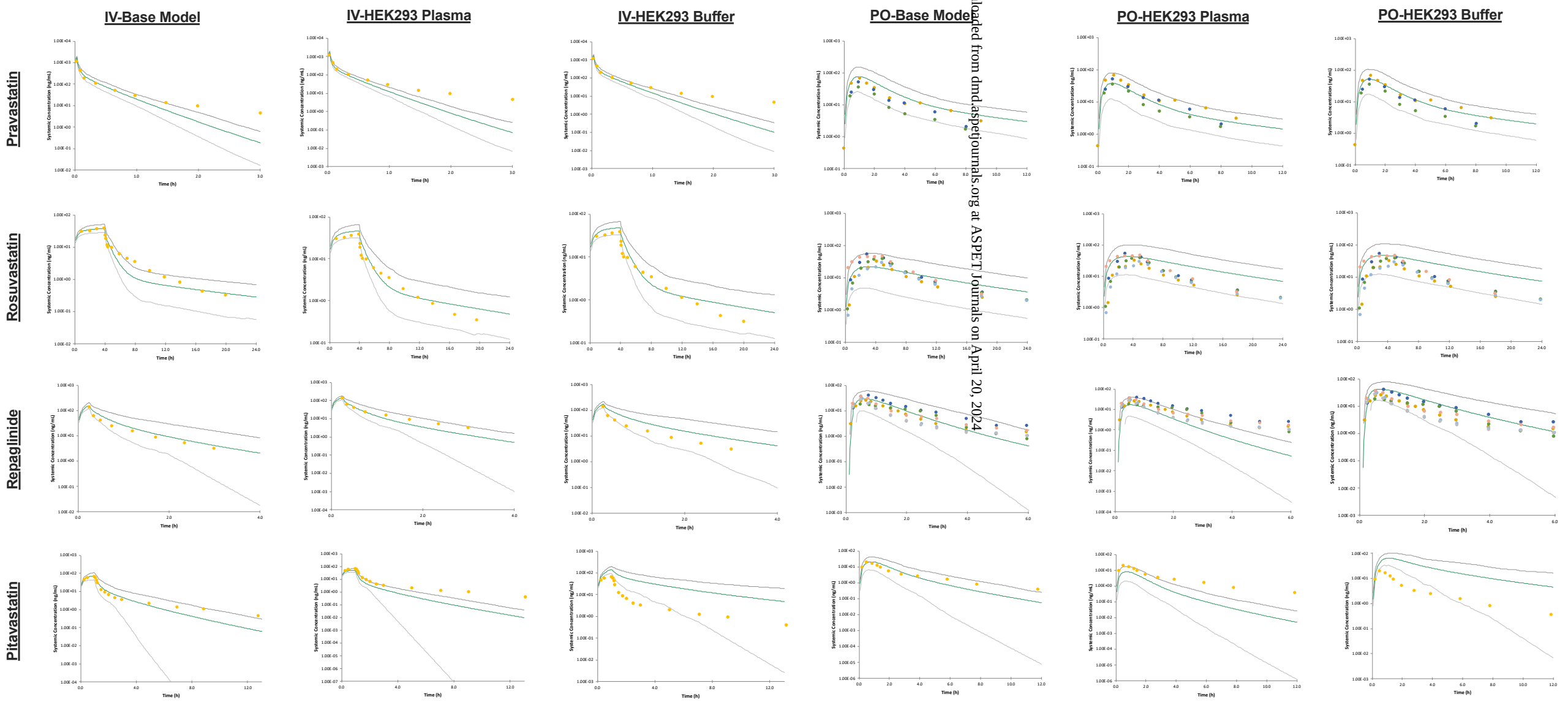

Figure 1

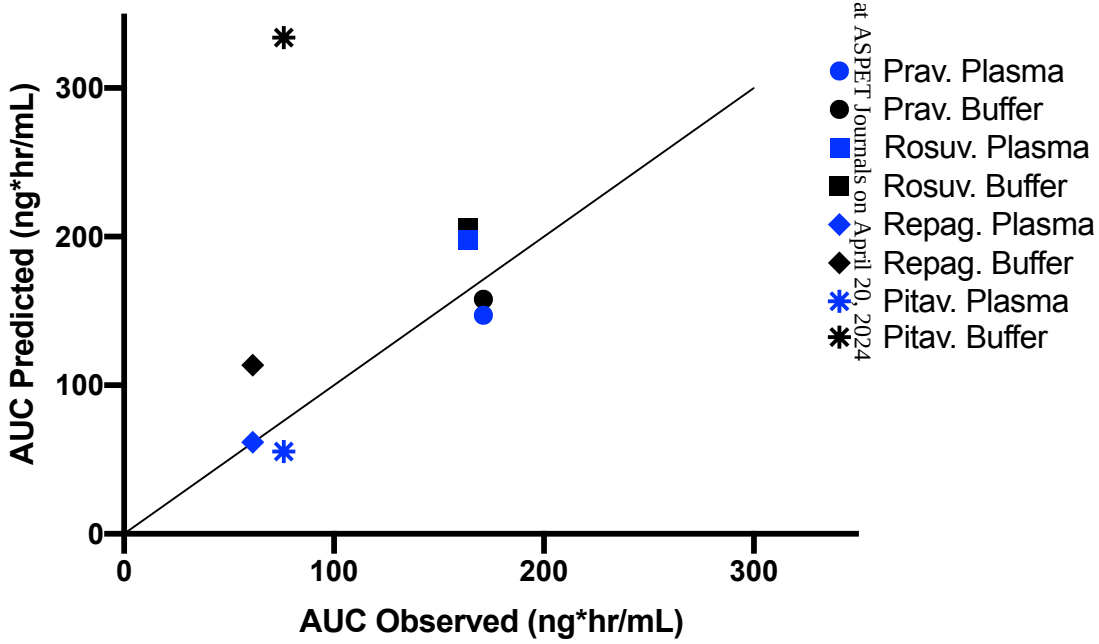

Figure 2